Loss of MARCH5 mitochondrial E3 ubiquitin ligase induces cellular senescence through dynamin-related protein 1 and mitofusin 1

Yong-Yea Park[1,2], Seungmin Lee[1,2], Mariusz Karbowski[3], Albert Neutzner[4], Richard J. Youle[4] and Hyeseong Cho[1,2,*]

[1]Department of Biochemistry, Ajou University School of Medicine, Yeongtong-gu, Suwon 443-721, Korea
[2]Graduate School of Molecular Science and Technology, Ajou University, Yeongtong-gu, Suwon 443-721, Korea
[3]University of Maryland Biotechnology Institute, Medical Biotechnology Center, Baltimore, MD 20892, USA
[4]Biochemistry Section, SNB, NINDS, National Institutes of Health, Bethesda, MD 20892, USA
*Author for correspondence (hscho@ajou.ac.kr)

Summary

Mitochondria constantly divide and combine through fission and fusion activities. MARCH5, a mitochondrial E3 ubiquitin ligase, has been identified as a molecule that binds mitochondrial fission 1 protein (hFis1), dynamin-related protein 1 (Drp1) and mitofusin 2 (Mfn2), key proteins in the control of mitochondrial fission and fusion. However, how these interactions control mitochondrial dynamics, and cellular function has remained obscure. Here, we show that shRNA-mediated MARCH5 knockdown promoted the accumulation of highly interconnected and elongated mitochondria. Cells transfected with MARCH5 shRNA or a MARCH5 RING domain mutant displayed cellular enlargement and flattening accompanied by increased senescence-associated β-galactosidase (SA-β-Gal) activity, indicating that these cells had undergone cellular senescence. Notably, a significant increase in Mfn1 level, but not Mfn2, Drp1 or hFis1 levels, was observed in MARCH5-depleted cells, indicating that Mfn1 is a major ubiquitylation substrate. Introduction of Mfn1^{T109A}, a GTPase-deficient mutant form of Mfn1, into MARCH5-RNAi cells not only disrupted mitochondrial elongation, but also abolished the increase in SA-β-Gal activity. Moreover, the aberrant mitochondrial phenotypes in MARCH5-RNAi cells were reversed by ectopic expression of Drp1, but not by hFis1, and reversion of the mitochondria morphology in MARCH5-depleted cells was accompanied by a reduction in SA-β-Gal activity. Collectively, our data indicate that the lack of MARCH5 results in mitochondrial elongation, which promotes cellular senescence by blocking Drp1 activity and/or promoting accumulation of Mfn1 at the mitochondria.

Key words: MARCH5, Cellular senescence, Mfn1, Drp1

Introduction

In most mammalian cell types, mitochondria form a highly dynamic reticular network that is controlled by a balance between mitochondrial fusion and fission events (Chan, 2006; Mozdy and Shaw, 2003). Several key molecules that control mitochondrial dynamics have been identified in mammals. The large GTPases mitofusin 1 and mitofusin 2 (Mfn1, Mfn2) are localized at the mitochondrial outer membrane and promote mitochondrial fusion (Chen et al., 2003; Ishihara et al., 2004; Santel and Fuller, 2001). Another dynamin-related GTPase, OPA1 (optic atrophy type 1), localized at the mitochondrial intermembrane space, cooperates with Mfn1 and Mfn2 during fusion events (Cipolat et al., 2004). For fission, mammalian cells require another GTPase, dynamin-related protein (Drp1), which interacts with the mitochondrial outer-membrane-anchored fission protein hFis1 (Suzuki et al., 2003). Most Drp1 is distributed throughout the cytoplasm; only a portion of cytosolic Drp1 is recruited to the mitochondria and interacts with hFis1 at the scission site (Yoon et al., 2003).

An imbalance between mitochondrial fission and fusion affects cellular physiology and has been directly linked to human diseases (Chen et al., 2007). Mutations in OPA1 and Mfn2 cause the neuronal diseases dominant optic atrophy type I and Charcot-Marie-Tooth neuropathy type 2a, respectively (Alexander et al., 2000; Delettre et al., 2000; Kijima et al., 2005; Zuchner et al., 2004). In addition,

fission defects resulting from a Drp1 mutation result in severe abnormal brain development and can be lethal (Waterham et al., 2007). Apoptotic processes are closely related to mitochondrial morphology control. Two pro-apoptotic regulators, Bax and Bak, can interact with the mitochondrial fission and fusion modulators Drp1 and mitofusins 1 and 2 (Brooks et al., 2007; Karbowski et al., 2002; Karbowski et al., 2006). Cells with fragmented mitochondria induced by knockdown of Mfn1 and/or Mfn2 or OPA1 are more vulnerable to apoptotic stimuli, whereas cells in which elongated mitochondria are maintained are resistant to extrinsic apoptotic damage (Lee et al., 2004; Yu et al., 2005). Interestingly, giant mitochondria found in aged cells and organisms are associated with reduced hFis1 expression (Yoon et al., 2006), and maintenance of elongated mitochondria by knockdown of hFis1 expression actively induced cellular senescence (Lee et al., 2007). Thus, one of the key questions in mitochondrial dynamics is how expression of mitochondrial fission and/or fusion molecules is controlled under different physiological or pathophysiological conditions.

Mitochondrial E3 ubiquitin ligases are involved in regulating mitochondrial dynamics (Karbowski et al., 2007; Nakamura et al., 2006; Yonashiro et al., 2006). Rsp5p was first identified as an ubiquitin ligase in *Saccharomyces cerevisiae*. Mutations in Rsp5p cause defects in mitochondrial morphology and distribution, demonstrating an essential role for this protein in mitochondrial

inheritance (Fisk and Yaffe, 1999). Fzo1 (*S. cerevisiae* mitofusin) is degraded by the proteosome following exposure to mating stimuli (Neutzner and Youle, 2005), and the F-box protein Mdm30 has been shown to be responsible for Fzo1 degradation (Cohen et al., 2008; Ota et al., 2008). A mitochondrial E3 ubiquitin ligase, membrane-associated RING-CH5 (MARCH5, also known as MITOL), has been discovered in mammals. MARCH5 localizes to the mitochondrial outer membrane and contains a RING-finger domain that is essential for ubiquitin transfer activity (Karbowski et al., 2007; Nakamura et al., 2006; Yonashiro et al., 2006). Interestingly, MARCH5 was reported to bind hFis1, Drp1 and Mfn2, and is responsible, in part, for ubiquitylation of these binding partners (Nakamura et al., 2006; Yonashiro et al., 2006). Earlier studies showed that the loss of MARCH5 enhanced mitochondria division, resulting in fragmented mitochondria (Nakamura et al., 2006; Yonashiro et al., 2006). By contrast, more recent data have shown that the functional loss of MARCH5 induced abnormal elongation and interconnection of mitochondria (Karbowski et al., 2007).

In this study, we attempted to clarify the ultimate consequence of MARCH5 loss on mitochondrial dynamics using a senescence model in which induction of elongated mitochondria, either by blocking mitochondrial fission or enhancing mitochondrial fusion, induces premature cellular senescence (Lee et al., 2007). Our results reveal that MARCH5-deficient cells undergo senescence in association with cellular changes that include abnormally elongated reticular mitochondria, indicating that a major role of MARCH5 in vivo is to facilitate mitochondrial division.

Results

Knockdown of MARCH5 results in elongated mitochondria and cellular senescence

MARCH5 was shown to interact with mitochondrial fission and fusion regulators, but the ultimate consequence of a lack of MARCH5 function has remained obscure (Karbowski et al., 2007; Nakamura et al., 2006; Yonashiro et al., 2006). We have recently reported that mitochondrial elongation is closely associated with the development of cellular senescence (Lee et al., 2007). Here, we hypothesized that if a lack of MARCH5 induces mitochondrial elongation, then the cells will undergo cellular senescence. We therefore depleted endogenous MARCH5 expression in HeLa and Chang cells by RNA interference (RNAi) using a short hairpin RNA (shRNA) insert targeting for endogenous MARCH5 mRNA. After transfections, cells were initially selected with 200 μg/ml hygromycin B and maintained in the presence of 30 μg/ml of hygromycin B (designated as day 0). Cells transfected with control shRNA retained the normal tubular spiral mitochondrial network (Fig. 1A, left panel) with relatively uniform thickness throughout the cytoplasm. By contrast, the mitochondria in cells expressing MARCH5 shRNA frequently exhibited a highly interconnected, even entangled, form with uneven thickness and a patchy subcellular distribution (Fig. 1A, right panel, and supplementary material Fig. S1) similar to those reported by Karbowski and colleagues (Karbowski et al., 2007). Approximately 60% of MARCH5 knockdown cells had such a highly interconnected mitochondrial structure, and the remaining cells showed a normal tubular mitochondrial structure, similar to that of control cells (Fig. 1C). We confirmed that knockdown of MARCH5 using the shRNA system was effective, showing that MARCH5 protein expression remained low even on day 5 (Fig. 1B).

Over time, MARCH5-depleted cells became flattened and exhibited an enlarged cellular morphology (Fig. 2A) reminiscent
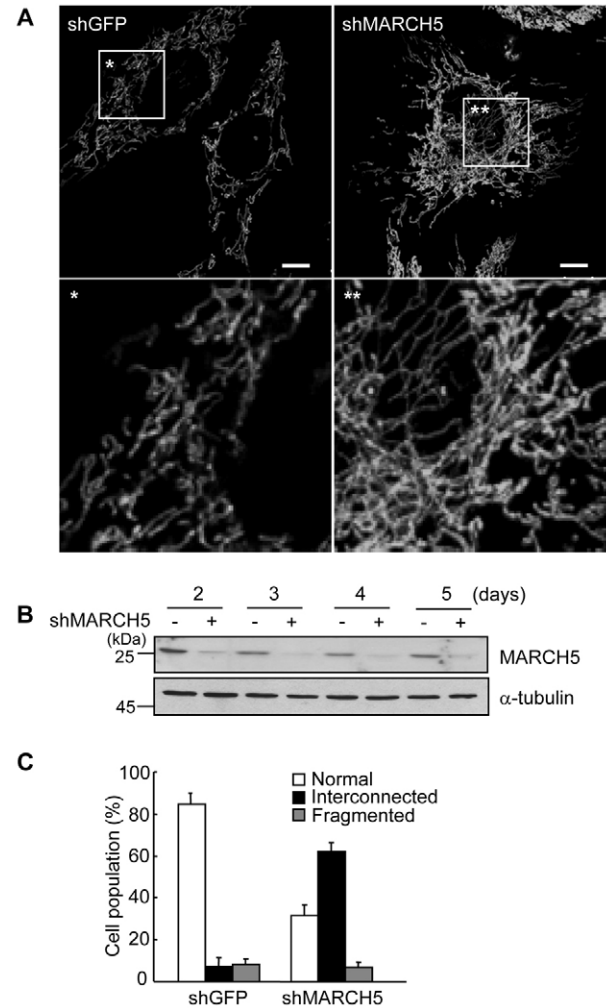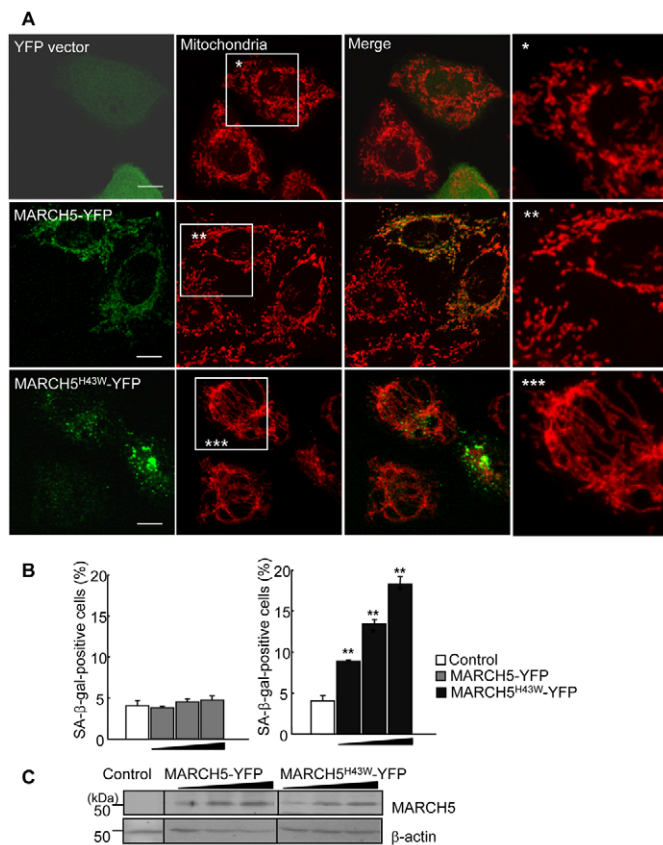

Fig. 1. Knockdown of MARCH5 expression induces mitochondrial elongation. Chang or HeLa cells were transfected with pREP4 vectors containing shRNA against MARCH5 target sequences (shMARCH5) or GFP target sequences (shGFP). The transfected cells were selected in 200 μg/ml of hygromycin B for 36 hours and then further grown in presence of 30 μg/ml of hygromycin B for up to 5 days. The first day of incubation with the lower concentration of hygromycin B was designated as day 0. (**A**) Mitochondrial morphology was visualized after staining with MitoTracker Red and images were captured under confocal microcopy. Lower panels show the boxed areas magnified for better resolution. Scale bars: 10 μm. (**B**) Cell lysates were obtained from days 2-5 and expression levels of MARCH5 protein determined by immunoblotting. (**C**) Percentage of cell population with fragmented, normal or highly interconnected (elongated) mitochondria. At least 250 cells in several fields were counted each day in two independent experiments.

of hFis1-depleted cells (Lee et al., 2007), suggesting that depletion of MARCH5 triggers cellular senescence. In fact, several senescence markers were apparently altered. A flow cytometric analysis showed that the 90° side-light scatter (90° LS) values, indicative of cellular granularity (Campisi, 2000), were higher by about twofold in the MARCH5-knockdown cells than in control cells on day 4 ($P<0.01$, Student's *t*-test; Fig. 2B). Likewise, the positive senescence-associated-β-galactosidase (SA-β-Gal) activity was apparent in flattened and enlarged cells lacking MARCH5 (Fig. 2C) and showed a threefold increase on day 4 ($P<0.01$, Student's *t*-test; Fig.
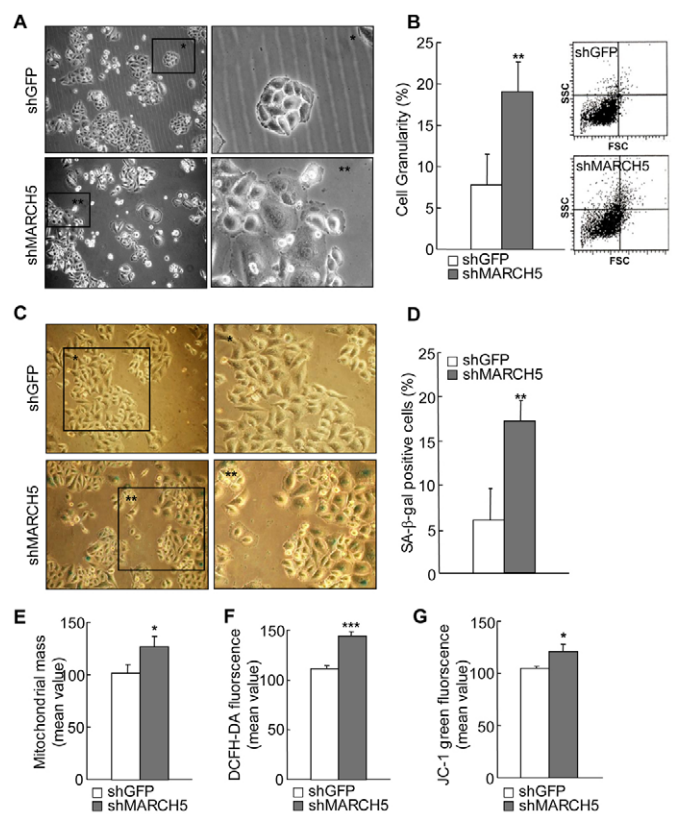
Fig. 2. MARCH5-deficient cells undergo cellular senescence. Chang cells were transfected with MARCH5 shRNA and the transfected cells were selected in the presence of hygromycin B. Several senescence-associated markers were analyzed on day 4. (**A**) Morphological changes were captured under phase-contrast microscopy. Boxed areas are magnified on the right. (**B**) Cellular granularity was evaluated by analyzing the 90° side-light scatter in flow cytometry. (**C**) On day 4, Chang cells were fixed with 2% formaldehyde in 0.2% glutaraldehyde solution, incubated with freshly prepared SA-β-gal staining solution for 36 hours and the images captured. Boxed areas are magnified on the right. (**D**) Quantification of SA-β-gal-positive cells. At least 300 cells were counted in several fields and data represent the average of four independent experiments. (**E**) Mitochondrial mass was measured after incubating cells with 125 nM of MitoTracker Red and quantified by flow cytometry. (**F**) To analyze intracellular ROS levels, cells were incubated with 10 µM H_2-DCFDA and the fluorescence intensities analyzed by flow cytometry. (**G**) Mitochondrial membrane potentials ($\Delta\psi_m$) were determined by incubating cells with 5 µg/ml of the JC-1 fluorescent dye. For quantification, the green fluorescence intensity (representing the degree of decreased $\Delta\psi_m$) was analyzed by flow cytometry in four independent experiments. *$P<0.05$, **$P<0.01$, ***$P<0.001$ vs control shRNA by Student's t-test.

Fig. 3. MARCH5 RING mutant induces mitochondrial elongation and cellular senescence. (**A**) HeLa cells were transfected with YFP vector, MARCH5-YFP and MARCH5 [H43W]-YFP. After incubation for 48 hours, cells were stained with MitoTracker Red and mitochondrial morphology analyzed by confocal microscopy. Boxed areas are magnified on the right. Scale bars: 10 µm. (**B**) Chang cells were transfected with increasing concentrations of MARCH5-YFP or MARCH5[H43W]-YFP expression vectors. At 48 hours post-transfection, cells were fixed and stained for SA-β-Gal activity. SA-β-Gal-positive cells were quantified. The results are the average of three independent experiments. (**C**) The expression levels of YFP vector, MARCH5-YFP and MARCH5[H43W]-YFP were analyzed by immunoblotting. *$P<0.05$, **$P<0.01$, ***$P<0.001$ vs control shRNA by Student's t-test.

2D). Consistent with this, other senescence-associated mitochondrial changes were accompanied in MARCH5-knockdown cells. Specifically, mitochondrial mass was increased and intracellular reactive oxygen species (ROS) levels were increased in MARCH5-depleted cells, together with a reduction in mitochondrial membrane potential ($\Delta\Psi m$) (Fig. 2E-G). Notably, mitochondrial DNA content and ATP levels were also reduced in these cells although reduction rates seemed to be less severe than those of hFis1-depleted cells (supplementary material Fig. S2A,B). Similarly, cell proliferation rate was retarded in MARCH5-depleted cells (supplementary material Fig. S2C). Collectively, these findings indicate that an imbalance between mitochondrial fission and fusion activities

induced by MARCH5 knockdown results in mitochondrial elongation, which in turn triggers cellular senescence.

Expression of a RING-domain mutant of MARCH5 increases positive SA-β-Gal staining

To determine whether the observed senescence-associated phenotypic changes in MARCH5-RNAi cells were the result of loss of MARCH5 function, we used the RING-domain mutant of MARCH5, MARCH5[H43W], in which ubiquitin transfer activity is predicted to be blocked due to replacement of the histidine residue in the Zn^{2+}-binding domain with tryptophan (Karbowski et al., 2007). Cells were transfected with YFP control vector, YFP-conjugated wild-type MARCH5 or the MARCH5[H43W] mutant and, after 48 hours, the changes in mitochondrial morphology and their potential correlation to senescent phenotypic changes were assessed. The levels of protein expression in cells transfected with wild-type and mutant MARCH5 constructs were comparable (Fig. 3C). To monitor senescent phenotypic changes, we stained for SA-β-Gal.

Of several available senescence markers, SA-β-Gal activity is the most widely used and is considered a reliable biochemical marker for senescence-associated phenotypic changes (Itahana et al., 2007; Patil et al., 2005). In green fluorescent cells expressing YFP-conjugated wild-type MARCH5 (MARCH5-YFP), mitochondrial morphology was indistinguishable from that in YFP control vector-transfected cells and neighboring untransfected cells (Fig. 3A), indicating that ectopic expression of wild-type MARCH5 did not significantly affect mitochondrial dynamics. Both YFP-tagged MARCH5 and Myc-tagged MARCH5 yielded similar results (data not shown), indicating that the YFP-tag does not interfere with the function of MARCH5. Overexpression of the MARCH5^{H43W} mutant (MARCH5^{H43W}-YFP), however, altered mitochondrial morphology: mitochondrial length was notably extended and mitochondria became increasingly entangled (Fig. 3A), effects that were similar to those observed in MARCH5-RNAi cells (Fig. 1 and supplementary material Fig. S1). Notably, dose-dependent increases in SA-β-Gal positivity were observed in cells transfected with MARCH5^{H43W} but not in cells transfected with wild-type MARCH5 (**$P<0.01$, ***$P<0.001$ Student's t-test; Fig. 3B). Thus, these data clearly demonstrate that the loss of MARCH5 function induced mitochondrial elongation that in turn triggered senescence-associated phenotypic changes.

Next, we confirmed that the observed senescence-associated phenotypic changes in MARCH5-depleted cells reflected functional changes in MARCH5 ubiquitin ligase activity. To accomplish this, we reintroduced MARCH5-R-YFP or MARCH5^{H43W}-R-YFP, resistant against MARCH5 shRNA-dependent degradation, into the cells transfected with MARCH5 shRNA and evaluated SA-β-Gal positivity 48 hours later. We found that reintroduction of MARCH5-R-YFP into MARCH5 RNAi cells restored MARCH5 expression (Fig. 4B) and caused a reduction of about 50% in SA-β-Gal staining (Fig. 4A). By contrast, introduction of MARCH5^{H43W}-R-YFP into the MARCH5 RNAi cells did not affect SA-β-Gal staining ($P<0.001$, Student's t-test; Fig. 4A), indicating that senescence-associated phenotypic changes in MARCH5-depleted cells are due to the loss of MARCH5 ubiquitin ligase activity. Using confocal microscopy, we confirmed the changes in mitochondrial morphology. MARCH5-RNAi cells coexpressing the control YFP vector exhibited highly interconnected mitochondria (Fig. 4C, upper panel). However, in cells expressing MARCH5-R-YFP, the mitochondria were less interconnected, and fragmented mitochondria were observed at the periphery of the cell (Fig. 4C, middle panel). By contrast, cells expressing MARCH5^{H43W}-R-YFP showed a mitochondrial morphology similar to that in neighboring MARCH5-depleted cells and there was no apparent increase in fragmented mitochondria (Fig. 4C, lower panel). Taken together, these data indicate that the loss of MARCH5 ubiquitin ligase activity induces abnormal mitochondrial elongation and senescence-associated phenotypic changes.

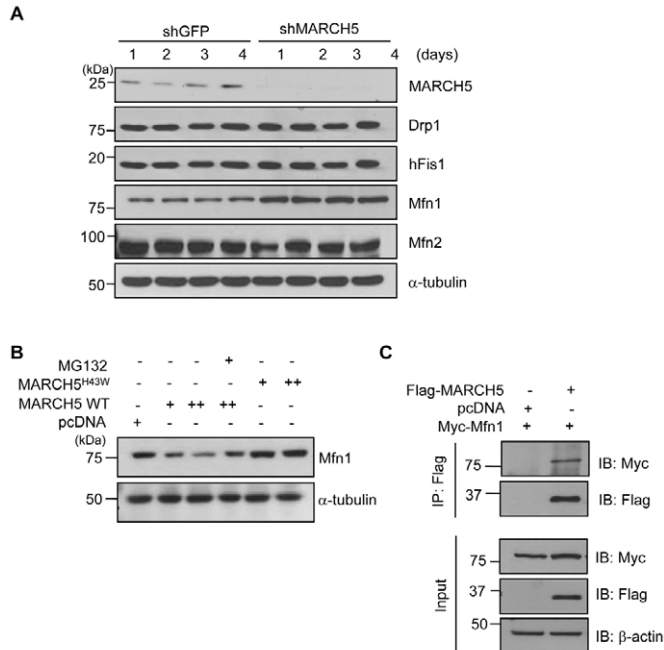### Mfn1 is a major ubiquitylation substrate of MARCH5

Because MARCH5 was shown to bind hFis1, Drp1 and Mfn2, we speculated that steady-state levels of its binding partners might be changed by MARCH5 depletion. Cell lysates were prepared from HeLa cells after switching to reduced concentrations of hygromycin B (days 1-4). Immunoblotting analysis showed a marked reduction in MARCH5 protein expression in MARCH5-shRNA cells (Fig. 5A). We observed that hFis1, Drp1 and Mfn2 levels were unchanged in MARCH5-depleted cells. Remarkably, however, Mfn1 levels were markedly increased in MARCH5-depleted cells, and
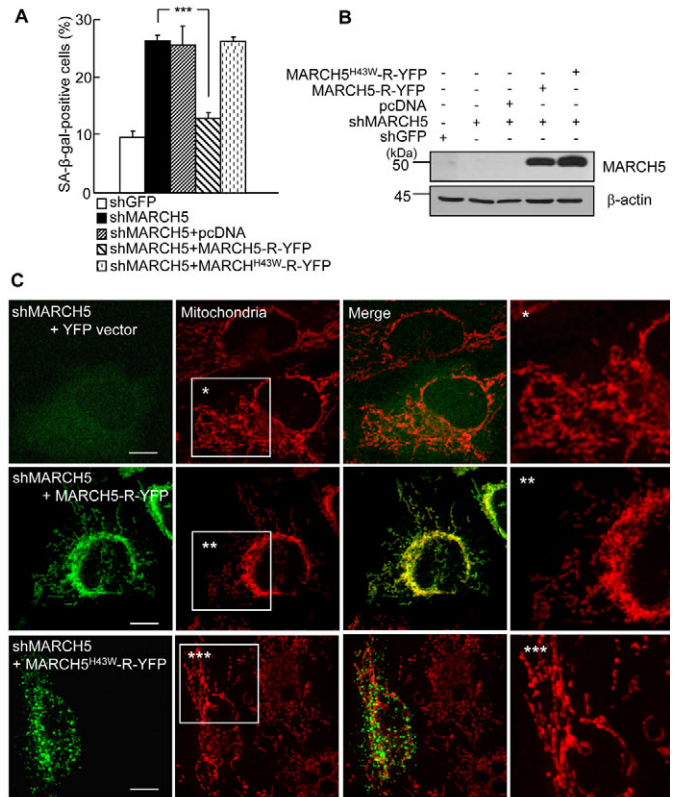
Fig. 4. Reintroduction of MARCH5 diminishes the number of SA-β-Gal-positive cells induced by MARCH5 depletion. MARCH5-R-YFP and MARCH5^{H43W}-R-YFP plasmids, which are resistant against MARCH5 shRNA, were transfected into the cells expressing MARCH5 shRNA on day 2. Two days post-transfection, cells were analyzed for the SA-β-Gal assay and mitochondrial morphology. (**A**) Quantification of SA-β-Gal-positive cells. Approximately 300 cells were counted in several fields and data represent the average of three independent experiments. ***$P<0.001$ vs MARCH5 shRNA by Student's t-test. (**B**) The expression levels of MARCH5-R-YFP and MARCH5^{H43W}-R-YFP were determined by immunoblotting. (**C**) Mitochondria were visualized with 125 nM MitoTracker Red staining and analyzed by confocal microscopy. Boxed areas are magnified on the right. Scale bars: 10 μm.

densitometry analysis revealed an approximately threefold increase in Mfn1 levels. To confirm the effect of MARCH5 on Mfn1 levels, we introduced MARCH5 and the MARCH5^{H43W} mutant into HeLa cells and determined Mfn1 levels. MARCH5, but not MARCH5^{H43W} lacking an E3 ligase activity, reduced the expression level of Mfn1, and the MARCH5-mediated degradation of Mfn1 was blocked in the presence of MG132, a proteasome inhibitor (Fig. 5B). Furthermore, using co-immunoprecipitation experiments, we found that MARCH5 interacts with Mfn1 (Fig. 5C). Thus, the data indicate that Mfn1 is a major ubiquitylation substrate of MARCH5.

If increased Mfn1 levels contribute to mitochondrial elongation and cellular senescence, abrogation of Mfn1 activity should prevent cellular senescence. To test this, we overexpressed Mfn1^{T109A}, a dominant-negative form of Mfn1 in which Thr109 (which is required for GTPase activity) was replaced with Ala, into the MARCH5-depleted cells. Ectopic expression of GFP-Mfn1^{T109A} induced a marked and significant increase in mitochondrial fragmentation in MARCH5-depleted cells, whereas neighboring
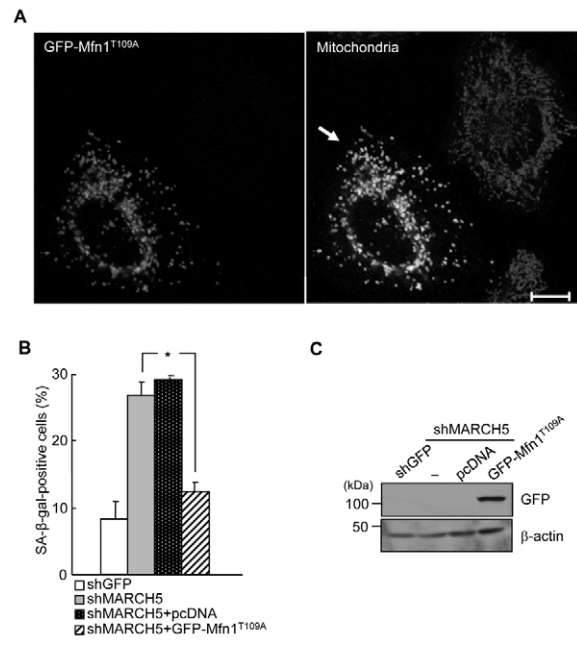
Fig. 5. Mfn1 is a major ubiquitylation substrate of MARCH5. (**A**) Control shRNA and MARCH5 shRNA were transfected into HeLa cells. The transfected cells were selected in 200 μg/ml of hygromycin B for 36 hours and then switched to a lower hygromycin B concentration for 4 days. Total cell lysates were obtained and expression levels of Mfn1, Mfn2, Drp1 and hFis1 proteins were determined by immunoblotting. (**B**) After HeLa cells were transfected with pcDNA, MARCH5 WT and MARCH5^{H43W} dose-dependently, cells were incubated with or without the proteasome inhibitor MG132 (20 μM) for 4 hours. The expression levels of Mfn1 were detected by immunoblotting from total cell lysates. (**C**) After HeLa cells were transfected with pcDNA, FLAG-MARCH5 and Myc-Mfn1, total cell lysates were immunoprecipitated with anti-FLAG antibody and the immunoprecipitates immunoblotted with anti-FLAG or anti-Myc antibody.
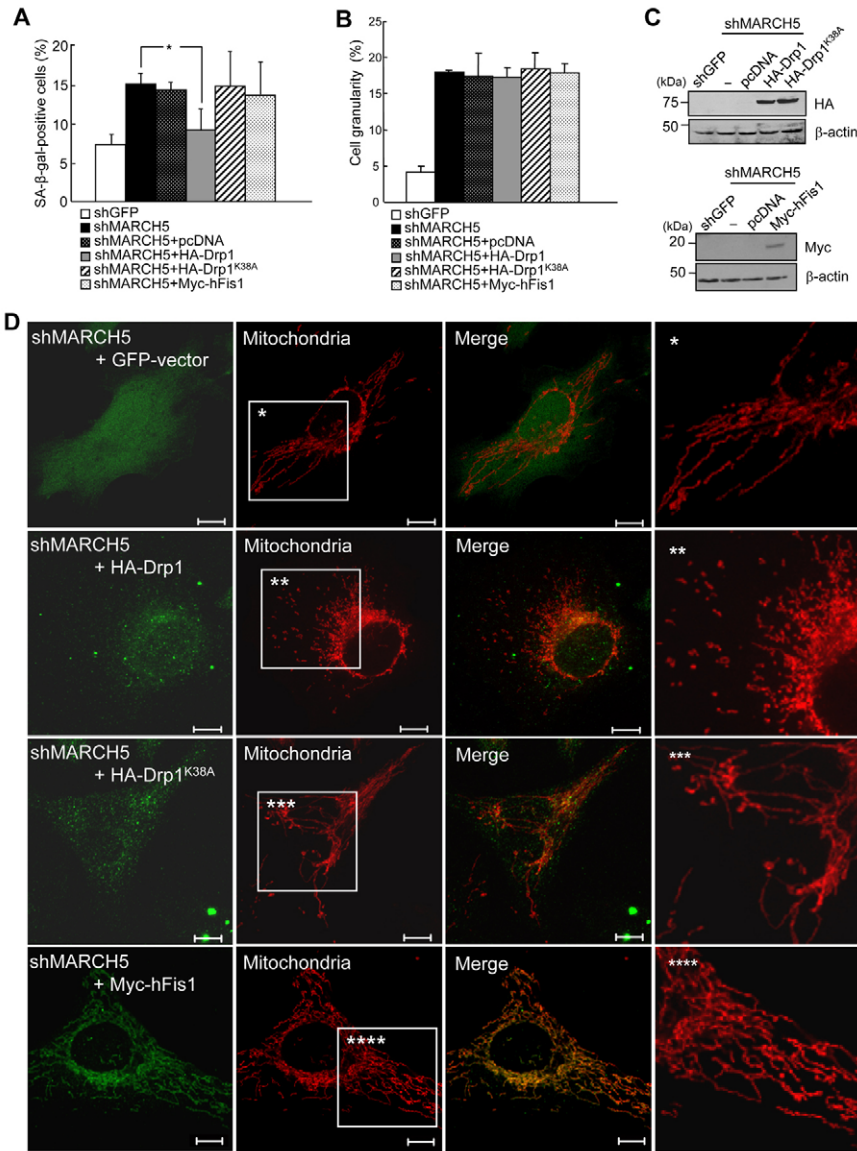
Fig. 6. Ectopic expressions of Mfn1^{T109A} diminish the SA-β-Gal positivity. The GFP-Mfn1^{T109A} expression vector was introduced into the MARCH5-depleted cells on day 2. After 2 days, cells were analyzed for SA-β-Gal activity and mitochondrial morphology. (**A**) Mitochondria were visualized after MitoTracker Red staining under confocal microscopy. Arrow indicates fragmented mitochondria. Scale bar: 10 μm. (**B**) Quantification of positive SA-β-Gal staining in ~ 300 cells each time in four independent experiments. *$P<0.05$ vs MARCH5 shRNA by Student's t-test. (**C**) The expression level of GFP-Mfn1^{T109A} was detected by immunoblotting using anti-GFP antibody.

MARCH5-depleted cells retained the interconnected mitochondrial morphology (Fig. 6A and supplementary material Fig. S3). Consequently, introduction of GFP-Mfn1^{T109A} into MARCH5-depleted cells caused a more than 50% reduction in SA-β-Gal staining ($P<0.05$, Student's t-test; Fig. 6B). This is the first indication that endogenous levels of Mfn1, but not Mfn2, are controlled by MARCH5 expression, and that the cellular senescence induced by MARCH5 depletion can be abrogated by the lack of fusion activity of Mfn1.

Introduction of Drp1 into MARCH5-depleted cells attenuates the level of SA-β-Gal staining

It was reported that MARCH5 binds Drp1 (Nakamura et al., 2006; Yonashiro et al., 2006), and more recently that ectopic expression of the MARCH5 RING-domain mutant hinders subcellular trafficking of Drp1 into the mitochondria (Karbowski et al., 2007). Therefore, Drp1 is another important downstream target of MARCH5. We therefore, introduced Drp1 into MARCH5-depleted cells and assessed transfected cells for reversion of senescence-associated phenotypic changes. The introduction of wild-type Drp1 into MARCH5-depleted cells significantly reduced the level of SA-β-Gal positivity ($P<0.05$, Student's t-test; Fig. 7A). By contrast, Drp1^{K38A}, a GTPase mutant of Drp1, had no effect. Moreover, unlike

Drp1, hFis1 overexpression in MARCH5-RNAi cells did not reduce the SA-β-Gal positivity, indicating that Drp1, but not hFis1, acts as a downstream mediator of MARCH5 activity. Close observation of mitochondrial morphology revealed that the addition of Drp1 into MARCH5-depleted cells disrupted the interconnection of mitochondria, whereas Drp1^{K38A} and hFis1 did not (Fig. 7D, supplementary material Fig. S4). We also assessed the ability of Drp1 and hFis1 to reverse the increase in cellular granularity observed in MARCH5-RNAi cells and found that neither overexpression of Drp1 nor hFis1 reduced the increased cellular granularity (Fig. 7B). Thus, inhibition of mitochondria elongation suppressed senescence-associated biochemical changes but not cellular changes. Collectively, these data indicate that the aberrant mitochondrial phenotypes in MARCH5-RNAi cells are reversed by ectopic expression of Drp1 and show that the reversion of mitochondrial morphology in MARCH5-depleted cells was accompanied by a reduction in SA-β-Gal activity.

Discussion

In this study, we identify a regulatory role for MARCH5 in mitochondrial dynamics and demonstrate a link between this activity and cellular function in mammalian cells. These data show that the loss of MARCH5 facilitates mitochondrial elongation and interconnection by at least two different mechanisms: (i) suppression of Drp1-mediated mitochondrial fission activity, probably through interruption of Drp1 subcellular trafficking (Karbowski et al., 2007), and (ii) a marked increase in the steady-state levels of Mfn1. The

Fig. 7. Ectopic expressions of Drp1 diminish the level of SA-β-Gal positivity induced by MARCH5 depletion. Hemagglutinin (HA)-Drp1, HA-Drp1^{K38A} and Myc-hFis1 expression vectors were introduced into the MARCH5-depleted cells on day 2. After 2 days, cells were analyzed for SA-β-Gal positivity, cellular granularity and mitochondrial morphology. (**A**) Quantification of SA-β-Gal-positive cells. Approximately 300 cells were counted in several fields and data represent the average of four independent experiments. **$P<0.01$ vs MARCH5 shRNA by Student's *t*-test. (**B**) Cellular granularity was evaluated by analyzing the side-light scatter in flow cytometry. (**C**) The ectopic expression levels of HA-Drp1, HA-Drp1^{K38A} and Myc-hFis1 were determined by immunoblotting. (**D**) Mitochondria were analyzed by confocal microscopy after staining with MitoTracker Red. Boxed areas are magnified on the right. Scale bars: 10 µm.

resulting highly interconnected reticular mitochondria impose a cellular stress that ultimately triggers cellular senescence.

MARCH5 was identified as a mitochondrial ubiquitin ligase that facilitates mitochondrial elongation (Nakamura et al., 2006; Yonashiro et al., 2006). The authors initially have shown that overexpression of MARCH5 promotes formation of elongated mitochondria. These studies also showed that MARCH5 interacts with hFis1, ubiquitylated Drp1 and Mfn2, and demonstrated that these interactions contribute to the degradation of MARCH5 binding partners (Nakamura et al., 2006; Yonashiro et al., 2006). Another study, however, reported that MARCH5 has the opposite effect on mitochondrial dynamics, showing that the loss of MARCH5 ubiquitin ligase activity or expression induced abnormally elongated and interconnected mitochondria rather than a fragmented form (Karbowski et al., 2007). Consistent with these latter results, we also observed that the loss of MARCH5 expression induced formation of highly interconnected and elongated mitochondria (Fig. 1). This high degree of mitochondrial interconnection might often lead to an uneven subcellular distribution of mitochondria that typically manifested as entangled

and perinuclearly aggregated mitochondria (supplementary material Fig. S1). Notably, the elongated form of mitochondria induced by MARCH5 knockdown is different from that in hFis1-depleted cells. As we have previously reported, the loss of hFis1 induced highly elongated mitochondria that stretched out uniformly throughout the cytoplasm (Lee et al., 2007). In MARCH5-depleted cells, a high degree of mitochondrial interconnection could be achieved by both a lack of Drp1 (Fig. 7), which reduced fission activity, and increased Mfn1 levels (Fig. 5), which enhanced fusion activity. It has been reported that the elongated mitochondria induced by Mfn1 overexpression often form perinuclear aggregates (Santel et al., 2003), supporting our observation in MARCH5-depleted cells (supplementary material Fig. S1). Molecular mechanisms defective of mitochondria fission activity differ in hFis1- and MARCH5-depleted cells. hFis1 levels in MARCH5-knockdown or MARCH5-RING mutant-expressed cells were not affected and must remain functional, but Drp1 activity at the mitochondria is crippled (Karbowski et al., 2007). Therefore, on the one hand, in MARCH5-knockdown cells defective of Drp1 activity, ectopic expression of Drp1, but not of hFis1, reversed the cellular phenotypic changes

(Fig. 7). On the other hand, in hFis1-knockdown cells, elongated mitochondria and senescence-associated phenotypic changes were triggered by lack of hFis1 and, therefore, ectopic expression of hFis1 (but not of Drp1) in those cells reversed the cellular phenotypic changes (Lee et al., 2007). Thus, a balance between mitochondrial fusion and fission activities, rather than specific mitochondria machinery components, precisely controls a variety of different mitochondrial morphologies and cellular phenotypes.

Because the steady-state level of Mfn1 in cells is dynamically controlled by endogenous MARCH5 expression, we propose that Mfn1 is a physiologically important target of MARCH5. hFis1, Drp1 and Mfn2 are reported to be major substrates of MARCH5; therefore, ubiquitylation of these target proteins is augmented by overexpression of MARCH5 (Nakamura et al., 2006; Yonashiro et al., 2006). However, whether the endogenous expression levels of these target proteins are regulated by overexpression or by depletion of MARCH5 in cells has not been demonstrated. Because we did not observe any changes in hFis1, Drp1 or Mfn2 expression in MARCH5-depleted cells (Fig. 5A), these interactions probably do not significantly affect mitochondrial dynamics at the physiological level. Indeed, we have found that Mfn1 interacts with MARCH5 and that degradation of Mfn1 occurs through a MARCH5-dependent ubiquitylation pathway (Fig. 5B,C).

As a result of the elongated mitochondrial morphology, the cells lacking MARCH5 experience cellular stress and undergo cellular senescence. Cellular senescence differs from replicative senescence and aging in that it can be induced by different stresses, including telomere shortening, DNA damage and oncogenic hyperactivation (Garinis et al., 2008; Stewart and Weinberg, 2006). Therefore, cellular senescence is referred to as stress-induced premature senescence. We previously demonstrated that abnormally elongated mitochondria per se, whether derived from lack of fission activity (hFis1 or Drp1 depletion) or enhanced fusion activity (Mfn1 or Opa1 overexpression), trigger stress-induced premature senescence (Lee et al., 2007). Stress-induced premature senescence shares several biochemical features with replicative senescence (Itahana et al., 2007; Patil et al., 2005). These include positive SA-β-Gal staining and increased ROS, accompanied by cellular morphological changes (Itahana et al., 2007; Patil et al., 2005). A significant increase in SA-β-Gal staining accompanied by increased ROS levels in MARCH5-depleted cells (Fig. 2, and supplementary material Fig. S2) clearly indicates that MARCH5 depletion facilitates the formation of elongated mitochondria, which cause cellular stress.

Several lines of recent evidence highlight the importance of post-translational modifications of regulatory molecules in the control of mitochondrial fusion and fission. Phosphorylation of Drp1 by protein kinase A (PKA) and Cdk1-cyclinB regulates Drp1 fission activity (Chang and Blackstone, 2007a; Chang and Blackstone, 2007b; Cribbs and Strack, 2007; Taguchi et al., 2007). In addition, sumoylation of Drp1 by conjugation of SUMO1 (small ubiquitin-related modifier 1) promotes recruitment and stabilization of Drp1 at the mitochondrial scission site, an event that occurs during apoptosis (Harder et al., 2004; Wasiak et al., 2007; Zunino et al., 2007). Ubiquitylation also regulates the expression levels of proteins that control mitochondrial dynamics through the 26S proteasome pathway and/or generates cellular signaling. In yeast, Fzo1 (Mfn homolog) is degraded following exposure to mating stimuli in a proteasome- (Neutzner and Youle, 2005) and Mdm30-dependent manner (Cohen et al., 2008; Ota et al., 2008). Here, we demonstrated that steady-state levels of Mfn1 can be controlled by MARCH5. Notably, another mitochondrial E3 ligase, MULAN, was described

as a NF-κB activator (Li et al., 2008; Matsuda et al., 2003). Thus, post-transcriptional modification and ubiquitin-dependent regulation in mitochondria must be central to controlling mitochondrial dynamics, which play an important role in cellular function.

In conclusion, we have shown that the mitochondrial ubiquitin ligase MARCH5 is actively involved in controlling mitochondrial dynamics through regulation of fission and fusion activities. Thus, loss of MARCH5 yielded highly interconnected, elongated mitochondria that triggered stress-induced cellular senescence. An intriguing question is whether MARCH5 expression or activity acts as an upstream regulator to control mitochondrial dynamics under physiological conditions other than senescence, including apoptosis and human diseases that involve mitochondrial dysfunction

Materials and Methods
Cell culture and transfections
Chang and HeLa cells were maintained in Dulbecco's modified Eagle's medium (DMEM; Invitrogen) supplemented with 10% heat-inactivated fetal bovine serum (FBS), 1% penicillin and streptomycin (GIBCO BRL) in a 5% CO_2 incubator at 37°C. Plasmid DNA transfections were carried out using polyethylenimine (PEI; Polysciences) as previously described (Lee et al., 2007). Briefly, DNA was mixed with PEI in a ratio of 1:2.5 and incubated in the presence of OPTI-MEM medium for 10 minutes at room temperature. The DNA complex was directly added to cells and incubated for 24-48 hours for transgene expression. For RNA interference, one day after transfection, cells were grown in the presence of 200 μg/ml hygromycin B (Roche Applied Science) for 2 days for selecting transfected cells. Dying cells were removed by brief centrifugation and the surviving cells reseeded on the plates (this time point was designated as day 0) and further grown in DMEM medium containing 30 μg/ml hygromycin B for up to 5 days (Karbowski et al., 2007; Lee et al., 2007).

RNA interference and plasmids
Silencing of endogenous MARCH5 mRNA was carried out using the short hairpin (sh)-activated gene silencing system as described (Karbowski et al., 2007). The MARCH5 shRNA plasmids were expressed under the pREP4 vector (Invitrogen) for long-term suppression of gene expression. To generate the MARCH5 expression vector resistant against MARCH5 shRNA, PCR was carried out with MARCH5-YFP as a template using the following primers: 5′-TCGAATTCCTGCAGAAGCCA-ATCCTTTA-3′ and 5′-GTGGATCCCGTGCTTCTTCTTGTTCTGGATAATT-3′). The resulting DNA fragments were cloned into the *Eco*RI and *Bam*HI site of MARCH5-YFP and MARCH5[H43W] to generate MARCH5-R-YFP and MARCH5[H43W]-R-YFP. Human MARCH5 WT (MARCH5-YFP) and MARCH5 RING mutant (MARCH5[H43W]-YFP) cloned into pYFP-N1 (BD Biosciences) expression vector described previously (Karbowski et al., 2007) were used. The hFis1 (Myc-hFis1 and GFP-hFis1) expression vectors were kindly provided by Mark A. McNiven (Mayo Clinic and Foundation, Rochester, MN) and Mfn1 (GFP-Mfn1[T109A]) expression vectors were provided by Margaret T. Fuller (Stanford University, Palo Alto, CA). The shRNAi of MARCH5 was performed as described previously (Karbowski et al., 2007; Lee et al., 2007).

Immunocytochemistry and confocal microscopy
The cells expressing MARCH5 RNAi plasmid after selection were seeded on coverslips and grown in the DMEM containing 30 μg/ml of hygromycin B. To visualize the mitochondria, 125 nM of MitoTracker Red (Molecular Probes) was added and incubated for 30 minutes. The cells were then fixed with 4% paraformaldehyde solution for 10 minutes and washed with a mixture of PBS and methanol (1:1). The fixed cells were permeabilized with methanol for 20 minutes at 20°C. For double immunofluorescence staining, cells were blocked with 1% bovine serum albumin in PBS for 1 hour at room temperature, followed by incubation with appropriate primary antibodies (anti-hemagglutinin and anti-c-Myc antibodies) overnight at 4°C, and subsequently probed with an Alexa-488-conjugated secondary antibody. For live-cell mitochondria imaging, cells were seeded in a coverglass-bottom dish (SPL Life Sciences, Gyeonggi-Do, Korea) in DMEM containing 30 μg/ml of hygromycin B. Mitochondria were stained with 100 nM of MitoTracker Green (Molecular Probes) for 30 minutes. Images were captured and analyzed using LSM510 confocal microscopy (Carl Zeiss).

Analysis of cellular granularity, ROS, ΔΨm, and mitochondrial mass
Increase in cellular granularity was quantified by analyzing the 90° side-light scatter in flow cytometry (FACS Vantage; BD Biosciences) (Lee et al., 2007). The change of ΔΨm was determined by quantifying the green fluorescence intensities (representing degree of ΔΨm disruption) after staining with 5 μg/ml of JC-1 (5,50,6,60-tetrachloro-1,10,3,30-tetraethylbenzimidazolylcarbocyanine iodide; Molecular Probes) in 5% CO_2 at 37°C for 20 minutes. Intracellular ROS levels were evaluated by incubating cells with 10 μM of 2′,7′-dichlorodihydrofluorescein diacetate (H2-DCFDA; Molecular Probes) fluorescence dye in 5% CO_2 at 37°C for 20 minutes. Changes in mitochondrial mass were determined by staining mitochondria with MitoTracker Red for 30 minutes.

All fluorescence intensities were quantified by flow cytometry (FACS Vantage). All results are the average of at least three independent experiments in triplicate.

Immunoblotting and antibodies

Total cell lysates were prepared by direct addition of $1\times$ SDS sample buffer to the culture dishes. The lysates were boiled, separated by SDS-PAGE and transferred to the polyvinylidene difluoride membrane (PVDF; Millipore). The immunoblots were visualized by enhanced chemiluminescence system (ECL; Amersham Biosciences). The MARCH5 antibodies were previously generated using recombinant full-length [HIS6]MARCH5 injected into a New Zealand White rabbit (Karbowski et al., 2007). Antibodies for hemagglutinin (1:1000) and c-Myc (1:1000) were purchased from Santa Cruz Biotechnology. Anti-Drp1 (1:1000; BD), anti-hFis1 (1:1000; Abcam) and anti-actin antibodies (1:2000; Sigma) were obtained.

Senescence-associated β-galactosidase assay

The selected cells in the presence of a high concentration of hygromycin B were seeded in a six-well plate in DMEM containing 30 µg/ml of hygromycin B for and incubated for various times. For SA-β-Gal assay, cells were washed with PBS and fixed in 2% formaldehyde dissolved in 0.2% glutaraldehyde solution for 10 minutes at room temperature. After fixation, cells were incubated with freshly prepared SA-β-Gal staining solution [40 mM citrate-phosphate buffer pH 6.0, 1 µg/ml 5-bromo-4-chloro-3-indolyl-β-D-galactosidase (X-Gal, Roche Applied Science), 5 mM potassium ferrocyanide, 5 mM potassium ferricyanide (Sigma), 150 mM NaCl, and 2 mM $MgCl_2$] at 37°C without CO_2 (Dimri et al., 1995). After incubation for 36 hours, SA-β-Gal-positive cells were counted under optical microscopy. The results are the average of at least three independent experiments.

Supplementary material available online at
http://jcs.biologists.org/cgi/content/full/123/4/619/DC1

References

Alexander, C., Votruba, M., Pesch, U. E., Thiselton, D. L., Mayer, S., Moore, A., Rodriguez, M., Kellner, U., Leo-Kottler, B., Auburger, G. et al. (2000). OPA1, encoding a dynamin-related GTPase, is mutated in autosomal dominant optic atrophy linked to chromosome 3q28. *Nat. Genet.* **26**, 211-215.

Brooks, C., Wei, Q., Feng, L., Dong, G., Tao, Y., Mei, L., Xie, Z. J. and Dong, Z. (2007). Bak regulates mitochondrial morphology and pathology during apoptosis by interacting with mitofusins. *Proc. Natl. Acad. Sci. USA* **104**, 11649-11654.

Campisi, J. (2000). Cancer, aging and cellular senescence. *In Vivo* **14**, 183-188.

Chan, D. C. (2006). Mitochondrial fusion and fission in mammals. *Annu. Rev. Cell Dev. Biol.* **22**, 79-99.

Chang, C. R. and Blackstone, C. (2007a). Cyclic AMP-dependent protein kinase phosphorylation of Drp1 regulates its GTPase activity and mitochondrial morphology. *J. Biol. Chem.* **282**, 21583-21587.

Chang, C. R. and Blackstone, C. (2007b). Drp1 phosphorylation and mitochondrial regulation. *EMBO Rep.* **8**, 1088-1089; author reply 1089-1090.

Chen, H., Detmer, S. A., Ewald, A. J., Griffin, E. E., Fraser, S. E. and Chan, D. C. (2003). Mitofusins Mfn1 and Mfn2 coordinately regulate mitochondrial fusion and are essential for embryonic development. *J. Cell Biol.* **160**, 189-200.

Chen, H., McCaffery, J. M. and Chan, D. C. (2007). Mitochondrial fusion protects against neurodegeneration in the cerebellum. *Cell* **130**, 548-562.

Cipolat, S., Martins de Brito, O., Dal Zilio, B. and Scorrano, L. (2004). OPA1 requires mitofusin 1 to promote mitochondrial fusion. *Proc. Natl. Acad. Sci. USA* **101**, 15927-15932.

Cohen, M. M., Leboucher, G. P., Livnat-Levanon, N., Glickman, M. H. and Weissman, A. M. (2008). Ubiquitin-proteasome-dependent degradation of a mitofusin, a critical regulator of mitochondrial fusion. *Mol. Biol. Cell* **19**, 2457-2464.

Cribbs, J. T. and Strack, S. (2007). Reversible phosphorylation of Drp1 by cyclic AMP-dependent protein kinase and calcineurin regulates mitochondrial fission and cell death. *EMBO Rep.* **8**, 939-944.

Delettre, C., Lenaers, G., Griffoin, J. M., Gigarel, N., Lorenzo, C., Belenguer, P., Pelloquin, L., Grosgeorge, J., Turc-Carel, C., Perret, E. et al. (2000). Nuclear gene OPA1, encoding a mitochondrial dynamin-related protein, is mutated in dominant optic atrophy. *Nat. Genet.* **26**, 207-210.

Dimri, G. P., Lee, X., Basile, G., Acosta, M., Scott, G., Roskelley, C., Medrano, E. E., Linskens, M., Rubelj, I., Pereira-Smith, O. et al. (1995). A biomarker that identifies senescent human cells in culture and in aging skin in vivo. *Proc. Natl. Acad. Sci. USA* **92**, 9363-9367.

Fisk, H. A. and Yaffe, M. P. (1999). A role for ubiquitination in mitochondrial inheritance in Saccharomyces cerevisiae. *J. Cell Biol.* **145**, 1199-1208.

Garinis, G. A., van der Horst, G. T., Vijg, J. and Hoeijmakers, J. H. (2008). DNA damage and ageing: new-age ideas for an age-old problem. *Nat. Cell Biol.* **10**, 1241-1247.

Harder, Z., Zunino, R. and McBride, H. (2004). Sumo1 conjugates mitochondrial substrates and participates in mitochondrial fission. *Curr. Biol.* **14**, 340-345.

Ishihara, N., Eura, Y. and Mihara, K. (2004). Mitofusin 1 and 2 play distinct roles in mitochondrial fusion reactions via GTPase activity. *J. Cell Sci.* **117**, 6535-6546.

Itahana, K., Campisi, J. and Dimri, G. P. (2007). Methods to detect biomarkers of cellular senescence: the senescence-associated beta-galactosidase assay. *Methods Mol. Biol.* **371**, 21-31.

Karbowski, M., Lee, Y. J., Gaume, B., Jeong, S. Y., Frank, S., Nechushtan, A., Santel, A., Fuller, M., Smith, C. L. and Youle, R. J. (2002). Spatial and temporal association of Bax with mitochondrial fission sites, Drp1, and Mfn2 during apoptosis. *J. Cell Biol.* **159**, 931-938.

Karbowski, M., Norris, K. L., Cleland, M. M., Jeong, S. Y. and Youle, R. J. (2006). Role of Bax and Bak in mitochondrial morphogenesis. *Nature* **443**, 658-662.

Karbowski, M., Neutzner, A. and Youle, R. J. (2007). The mitochondrial E3 ubiquitin ligase MARCH5 is required for Drp1 dependent mitochondrial division. *J. Cell Biol.* **178**, 71-84.

Kijima, K., Numakura, C., Izumino, H., Umetsu, K., Nezu, A., Shiiki, T., Ogawa, M., Ishizaki, Y., Kitamura, T., Shozawa, Y. et al. (2005). Mitochondrial GTPase mitofusin 2 mutation in Charcot-Marie-Tooth neuropathy type 2A. *Hum. Genet.* **116**, 23-27.

Lee, S., Jeong, S. Y., Lim, W. C., Kim, S., Park, Y. Y., Sun, X., Youle, R. J. and Cho, H. (2007). Mitochondrial fission and fusion mediators, hFis1 and OPA1, modulate cellular senescence. *J. Biol. Chem.* **282**, 22977-22983.

Lee, Y. J., Jeong, S. Y., Karbowski, M., Smith, C. L. and Youle, R. J. (2004). Roles of the mammalian mitochondrial fission and fusion mediators Fis1, Drp1, and Opa1 in apoptosis. *Mol. Biol. Cell* **15**, 5001-5011.

Li, W., Bengtson, M. H., Ulbrich, A., Matsuda, A., Reddy, V. A., Orth, A., Chanda, S. K., Batalov, S. and Joazeiro, C. A. (2008). Genome-wide and functional annotation of human E3 ubiquitin ligases identifies MULAN, a mitochondrial E3 that regulates the organelle's dynamics and signaling. *PLoS ONE* **3**, e1487.

Matsuda, A., Suzuki, Y., Honda, G., Muramatsu, S., Matsuzaki, O., Nagano, Y., Doi, T., Shimotohno, K., Harada, T., Nishida, E. et al. (2003). Large-scale identification and characterization of human genes that activate NF-kappaB and MAPK signaling pathways. *Oncogene* **22**, 3307-3318.

Mozdy, A. D. and Shaw, J. M. (2003). A fuzzy mitochondrial fusion apparatus comes into focus. *Nat. Rev. Mol. Cell. Biol.* **4**, 468-478.

Nakamura, N., Kimura, Y., Tokuda, M., Honda, S. and Hirose, S. (2006). MARCH-V is a novel mitofusin 2- and Drp1-binding protein able to change mitochondrial morphology. *EMBO Rep.* **7**, 1019-1022.

Neutzner, A. and Youle, R. J. (2005). Instability of the mitofusin Fzo1 regulates mitochondrial morphology during the mating response of the yeast Saccharomyces cerevisiae. *J. Biol. Chem.* **280**, 18598-18603.

Ota, K., Kito, K., Okada, S. and Ito, T. (2008). A proteomic screen reveals the mitochondrial outer membrane protein Mdm34p as an essential target of the F-box protein Mdm30p. *Genes Cells* **13**, 1075-1085.

Patil, C. K., Mian, I. S. and Campisi, J. (2005). The thorny path linking cellular senescence to organismal aging. *Mech. Ageing. Dev.* **126**, 1040-1045.

Santel, A. and Fuller, M. T. (2001). Control of mitochondrial morphology by a human mitofusin. *J. Cell Sci.* **114**, 867-874.

Santel, A., Frank, S., Gaume, B., Herrler, M., Youle, R. J. and Fuller, M. T. (2003). Mitofusin-1 protein is a generally expressed mediator of mitochondrial fusion in mammalian cells. *J. Cell Sci.* **116**, 2763-2774.

Stewart, S. A. and Weinberg, R. A. (2006). Telomeres: cancer to human aging. *Annu. Rev. Cell Dev. Biol.* **22**, 531-557.

Suzuki, M., Jeong, S. Y., Karbowski, M., Youle, R. J. and Tjandra, N. (2003). The solution structure of human mitochondria fission protein Fis1 reveals a novel TPR-like helix bundle. *J. Mol. Biol.* **334**, 445-458.

Taguchi, N., Ishihara, N., Jofuku, A., Oka, T. and Mihara, K. (2007). Mitotic phosphorylation of dynamin-related GTPase Drp1 participates in mitochondrial fission. *J. Biol. Chem.* **282**, 11521-11529.

Wasiak, S., Zunino, R. and McBride, H. M. (2007). Bax/Bak promote sumoylation of DRP1 and its stable association with mitochondria during apoptotic cell death. *J. Cell Biol.* **177**, 439-450.

Waterham, H. R., Koster, J., van Roermund, C. W., Mooyer, P. A., Wanders, R. J. and Leonard, J. V. (2007). A lethal defect of mitochondrial and peroxisomal fission. *N. Engl. J. Med.* **356**, 1736-1741.

Yonashiro, R., Ishido, S., Kyo, S., Fukuda, T., Goto, E., Matsuki, Y., Ohmura-Hoshino, M., Sada, K., Hotta, H., Yamamura, H. et al. (2006). A novel mitochondrial ubiquitin ligase plays a critical role in mitochondrial dynamics. *EMBO J.* **25**, 3618-3626.

Yoon, Y., Krueger, E. W., Oswald, B. J. and McNiven, M. A. (2003). The mitochondrial protein hFis1 regulates mitochondrial fission in mammalian cells through an interaction with the dynamin-like protein DLP1. *Mol. Cell. Biol.* **23**, 5409-5420.

Yoon, Y. S., Yoon, D. S., Lim, I. K., Yoon, S. H., Chung, H. Y., Rojo, M., Malka, F., Jou, M. J., Martinou, J. C. and Yoon, G. (2006). Formation of elongated giant mitochondria in DFO-induced cellular senescence: involvement of enhanced fusion process through modulation of Fis1. *J. Cell Physiol.* **209**, 468-480.

Yu, T., Fox, R. J., Burwell, L. S. and Yoon, Y. (2005). Regulation of mitochondrial fission and apoptosis by the mitochondrial outer membrane protein hFis1. *J. Cell Sci.* **118**, 4141-4151.

Zuchner, S., Mersiyanova, I. V., Muglia, M., Bissar-Tadmouri, N., Rochelle, J., Dadali, E. L., Zappia, M., Nelis, E., Patitucci, A., Senderek, J. et al. (2004). Mutations in the mitochondrial GTPase mitofusin 2 cause Charcot-Marie-Tooth neuropathy type 2A. *Nat. Genet.* **36**, 449-451.

Zunino, R., Schauss, A., Rippstein, P., Andrade-Navarro, M. and McBride, H. M. (2007). The SUMO protease SENP5 is required to maintain mitochondrial morphology and function. *J. Cell Sci.* **120**, 1178-1188.